

N-terminal truncated peroxisome proliferator-activated receptor- γ coactivator-1 α alleviates phenylephrine-induced mitochondrial dysfunction and decreases lipid droplet accumulation in neonatal rat cardiomyocytes

ZUHENG LIU^{1,2*}, JINGHAI HUA^{1,2*}, WANQIANG CAI^{1,2}, QIONG ZHAN^{1,2},
WENYAN LAI^{1,2}, QINGCHUN ZENG^{1,2}, HAO REN^{2,3} and DINGLI XU^{1,2}

¹State Key Laboratory of Organ Failure Research, Department of Cardiology, Nanfang Hospital, Southern Medical University;

²Key Laboratory for Organ Failure Research, Ministry of Education of The People's Republic of China;

³Department of Rheumatology, Nanfang Hospital, Southern Medical University,
Guangzhou, Guangdong 510515, P.R. China

Received November 24, 2017; Accepted April 30, 2018

DOI: 10.3892/mmr.2018.9158

Abstract. N-terminal truncated peroxisome proliferator-activated receptor- γ coactivator-1 α (NT-PGC-1 α) is an alternative splice variant of PGC-1 α . NT-PGC-1 α exhibits stronger anti-obesity effects in adipose tissue than PGC-1 α ; however, NT-PGC-1 α has not yet been investigated in neonatal rat cardiomyocytes (NRCMs). The present study aimed to investigate the role of NT-PGC-1 α in mitochondrial fatty acid metabolism and its possible regulatory mechanism in NRCMs. NRCMs were exposed to phenylephrine (PE) or angiotensin II (Ang II) to induce cardiac hypertrophy. Following this, NRCMs were infected with adenovirus expressing NT-PGC-1 α , and adenosine 5'-triphosphate (ATP) levels, reactive oxygen species (ROS) generation and mitochondrial membrane potential were subsequently detected. In addition, western blotting, lipid droplet staining and oxygen consumption assays were performed to examine the function of NT-PGC-1 α in fatty acid metabolism. NT-PGC-1 α was demonstrated to be primarily

expressed in the cytoplasm, which differed from full-length PGC-1 α , which was predominantly expressed in the nucleus. NT-PGC-1 α overexpression alleviated mitochondrial function impairment, including ATP generation, ROS production and mitochondrial membrane potential integrity. Furthermore, NT-PGC-1 α overexpression alleviated the PE-induced suppression of fatty acid metabolism-associated protein expression, increased extracellular oxygen consumption and decreased lipid droplet accumulation in NRCMs. Taken together, the present study demonstrated that NT-PGC-1 α alleviated PE-induced mitochondrial impairment and decreased lipid droplet accumulation in NRCMs, indicating that NT-PGC-1 α may have ameliorated mitochondrial energy defects in NRCMs, and may be considered as a potential target for the treatment of heart failure.

Introduction

Heart failure is thought to be comparable to an engine that has run out of fuel, due to the key involvement of mitochondrial dysfunction (1). Therefore, improving the cellular energy supply may provide a promising therapeutic strategy for individuals with heart failure. Peroxisome proliferator-activated receptor (PPAR)- γ coactivator-1 α (PGC-1 α), a major regulator of energy metabolism, is abundantly expressed in the mitochondria and initiates multiple responses, including adaptive thermogenesis (2), fatty acid oxidation (FAO) (3) and mitochondrial biogenesis (4). Thus, PGC-1 α may be a candidate target for the treatment of heart disease, as fatty acid metabolism supplies more adenosine 5'-triphosphate (ATP) than carbohydrate metabolism (5). Furthermore, as FAO is decreased when heart failure or cardiac hypertrophy emerges, strategies promoting the re-utilization of fatty acids by the heart appear to be a promising therapeutic approach for the treatment of heart failure (6).

PGC-1 α inactivation impairs cardiac output in isolated working hearts or cardiac responses in transgenic mice

Correspondence to: Professor Dingli Xu, State Key Laboratory of Organ Failure Research, Department of Cardiology, Nanfang Hospital, Southern Medical University, 1838 Northern Guangzhou Avenue, Guangzhou, Guangdong 510515, P.R. China
E-mail: dinglixu@fimmu.com

Professor Hao Ren, Department of Rheumatology, Nanfang Hospital, Southern Medical University, 1838 Northern Guangzhou Avenue, Guangzhou, Guangdong 510515, P.R. China
E-mail: renhao67@aliyun.com

*Contributed equally

Key words: N-terminal truncated peroxisome proliferator-activated receptor- γ coactivator-1 α , peroxisome proliferator-activated receptor- α , neonatal rat cardiomyocytes, mitochondria, fatty acid, metabolism

challenged with physiological stress, and ultimately contributes to increased mortality in response to stress (7-9). By contrast, PGC-1 α overexpression enhances mitochondrial biogenesis by increasing oxygen consumption and ATP production (3,10). However, constitutive PGC-1 α overexpression leads to abnormal mitochondrial genesis and cardiomyopathy (11). This outcome is abolished by decreasing PGC-1 α expression to basal levels (11). Although PGC-1 α overexpression results in cardiac function deterioration in a mouse model of transverse aortic constriction (TAC) (9), Pereira *et al* (12) demonstrated that the use of a transgene to maintain PGC-1 α expression in TAC mice preserves angiogenic function rather than contractile and mitochondrial functions. However, investigation in cardiomyocytes indicated that the expression of full-length PGC-1 α (FL-PGC-1 α) is downregulated in the presence of pro-hypertrophic factors such as high-glucose and angiotensin (Ang) II, and may be involved in autophagy and anti-inflammatory processes (13,14). Despite the beneficial effects reported by certain studies, further study is required to determine whether increasing PGC-1 α expression under pathological conditions has a favorable impact (15,16). In addition, various subtypes of PGC-1 α have not been fully investigated; therefore, the present study aimed to explore the function of N-terminal truncated PGC-1 α (NT-PGC-1 α) in cardiomyocytes.

NT-PGC-1 α is an alternative splice variant of full-length PGC-1 α that contains the first 270 amino acids of the full-length protein (17). NT-PGC-1 α has a longer half-life than PGC-1 α and is predominantly located in the cytoplasm (18,19). NT-PGC-1 α is sensitive to oxidative stress, and is downregulated in the brains of patients with diabetes and Alzheimer's disease (20). However, the function of NT-PGC-1 α in cardiomyocytes remains unclear. In the present study, NT-PGC-1 α was suggested as a metabolic regulator in neonatal rat cardiomyocytes (NRCMs). It was demonstrated that NT-PGC-1 α activated fatty acid metabolism-associated downstream molecules, prevented a decrease in mitochondrial membrane potential and ATP concentration, reduced reactive oxygen species (ROS) generation, decreased lipid droplet accumulation and increased oxygen consumption. This suggested that NT-PGC-1 α may be beneficial in mitochondrial impairment prevention and may be involved in mitochondrial fatty acid metabolism. Thus, NT-PGC-1 α represents a potential therapeutic target in heart failure.

Materials and methods

Experimental animals. Neonatal Sprague-Dawley rats (1-3 days old) were obtained from the Laboratory Animal Center of Southern Medical University (Guangzhou, China) and sacrificed immediately. The present study was approved by the Southern Medical University review board and the animal protocols used complied with the Guide for the Care and Use of Laboratory Animals (21).

Isolation and culture of NRCMs. Neonatal Sprague-Dawley rats were sacrificed via 2% isoflurane inhalation and subsequent cervical dislocation. Hearts were removed, dissected and enzymatically digested with 0.2% pancreatin overnight at 4°C. Cells were subsequently isolated by magnetic stirring with collagenase II (1 mg/ml) in a sterile glass vial. Following

90 min of differential adhesion at 37°C, isolated cells were plated in a culture dish in the presence of 0.1 mM 5-bromo-2'-deoxyuridine (BrdU; Sigma-Aldrich; Merck KGaA, Darmstadt, Germany) to inhibit fibroblast proliferation with 10% fetal bovine serum (Gibco; Thermo Fisher Scientific, Inc., Waltham, MA, USA) in Dulbecco's modified Eagle's medium (DMEM) medium (Gibco; Thermo Fisher Scientific, Inc.). Following 48 h at 37°C, spontaneously contracting NRCMs were treated with 10 μ M phenylephrine (PE; Selleck Chemicals, Shanghai, China) for 48 h at 37°C, 1 μ M Ang II (Abcam, Cambridge, MA, USA) for 24 h, JC-1 (Beyotime Institute of Biotechnology, Haimen, China) for 20 min or 4,4-difluoro-5,7-dimethyl-4-bora-3a,4a-diaza-*s*-indacene-3-dodecanoic acid (BODIPYTM FL C₁₂) lipid probe (Thermo Fisher Scientific, Inc.) for 30 min in DMEM containing penicillin and streptomycin (100:1) (Gibco; Thermo Fisher Scientific, Inc.) without FBS. PE and Ang II are pro-hypertrophic factors that were applied to induce cardiac hypertrophy. JC-1 is a probe used to detect the mitochondrial membrane potential and FL-C₁₂ is used to measure the lipid accumulation in cells.

Reverse transcription-quantitative polymerase chain reaction (RT-qPCR). The protocols used for RT-qPCR were in accordance with the manufacturer's guidelines. Briefly, total RNA from NRCMs was extracted using RNAiso Plus (Takara Biotechnology Co., Ltd., Dalian, China). Total RNA (1 μ g/reaction) was reverse transcribed to cDNA with reverse transcriptase and random hexamer primers (PrimeScriptTM RT reagent kit with gDNA Eraser, Takara Biotechnology Co., Ltd.). RT was conducted at 37°C for 15 min, 85°C for 5 sec and stop at 4°C. qPCR was conducted at 95°C 15 sec for 1 cycle, 95°C 5 sec and 60°C for 5 sec under 40 cycles, using synthesized cDNA in a 10 μ l reaction volume (SYBR Green PCR kit; Takara Biotechnology Co., Ltd.) with a LightCycler 480 system (Roche Diagnostics, Basel, Switzerland). Gene expression levels were normalized to β -actin and quantified using the 2^{- $\Delta\Delta$ C_q} method (22). The primers used are listed in Table I (Sangon Biotech Co., Ltd., Shanghai, China).

Recombinant adenovirus infection. Recombinant adenoviruses including mCherry-NT-PGC-1 α and NT-PGC-1 α (virus titer: 9x10⁹ cfu/ml) were purchased from Obio Technology Corp., Ltd. (Shanghai, China). Overexpression of NT-PGC-1 α in NRCMs was achieved by infection with the recombinant adenovirus at a multiplicity of infection (MOI) of 100 (cells were at a density of 1.5x10⁶ in 60-mm plate). Following 4 h of infection at 37°C, an equal volume of fresh DMEM with 10% FBS was added to the culture. The cells were incubated for a further 24 h at 37°C to allow the virus to achieve maximum effect. The corresponding vehicle control were adenoviruses without NT-PGC-1 α .

Immunofluorescence. NRCMs were washed with PBS and fixed with 4% paraformaldehyde for 15 min at 4°C. Following a further wash, cells were blocked with a 1% goat serum albumin (Beyotime Institute of Biotechnology, Haimen, China) for 1 h and permeabilized in PBS with 0.1% Triton X-100 for 5 min at room temperature. Anti-PGC-1 α -N-terminal antibody (1:100; cat. no. ab191838; Abcam) was applied overnight

Table I. Primer sequences used for reverse transcription-quantitative polymerase chain reaction.

| Gene | Forward primer (5'-3') | Reverse primer (5'-3') |
|-------------------|------------------------|------------------------|
| β -actin | TGGACAGTGAGGCAAGGATAG | TACTGCCCTGGCTCCTAGCA |
| Acadm | GTCGCCCCAGACTACGATAA | GCCAAGACCACCACAACCTCT |
| Acadv1 | TGGACAAAGGAAAGGAAGTCA | ACTCAGACCACTGCCAATCC |
| PDK4 | ACCGTCGTCCTGGGAAAAG | CGTTGGAGCAGTGGAGTATG |
| CPT1B | AAGAACACGAGCCAACAAGC | TACCATACCCAGTGCCATCA |
| CPT-2 | CTGTCCACCAGCACTCTGAA | GCAGCCTATCCAGTCATCGT |
| SOD2 | CTGGCTTGGCTTCAATAAGG | CGTGCTCCCACACATCAAT |
| SOD3 | TCTGCAACCTGCTACTGGTG | AGTGCGTGTGCGCCTATCTTC |
| PPAR- α | GACAAGGCCTCAGGATACCA | TCTTGCAGCTTCGATCACAC |
| NT-PGC-1 α | ACCACAAACGATGACCCTCC | CTGCGGTTGTGTATGGGACT |
| FL-PGC-1 α | GGCACGCAGTCTTATTCATT | CATCCTTTGGGGTCTTTGAG |

Acadm, medium-chain specific acyl-CoA dehydrogenase, mitochondrial; Acadv1, acyl-coenzyme A dehydrogenase-very long chain; PDK4, pyruvate dehydrogenase kinase 4; CPT1B, carnitine palmitoyltransferase 1b; CPT-2, carnitine palmitoyltransferase 2; SOD, superoxide dismutase; PPAR, peroxisome proliferator-activated receptor; NT, N-terminal truncated; FL, full length; PGC-1 α , PPAR- γ coactivator-1 α .

at 4°C. Fluorescein isothiocyanate-conjugated goat anti-rabbit immunoglobulin G (IgG) secondary antibody (1:200; cat. no. sc-2012; Santa Cruz Biotechnology, Inc., Dallas, TX, USA) was subsequently added for 2 h at room temperature. For the visualization of nuclei, cells fixed at 4°C were incubated with DAPI for 10 min at room temperature. In addition, live cells were infected with mCherry-NT-PGC-1 α or mCherry adenovirus and incubated with Hoechst 33258 for 10 min. Cells were observed under a confocal microscope (Olympus FV10i' magnifications, x10 or 60).

Western blot analysis. Protein was extracted from cultured NRCMs using radioimmunoprecipitation assay lysis buffer (Beyotime Institute of Biotechnology) containing protease inhibitors (1:100; Sigma-Aldrich; Merck KGaA) and quantified with a bicinchoninic acid (BCA) protein assay. Total nuclear and cytoplasmic protein was separated using a Nuclear and Cytoplasmic Extraction Reagent kit (Thermo Fisher Scientific, Inc.). Equal amounts of cell lysates (30 μ g/lane) were determined via a Bicinchoninic Acid protein assay (Thermo Fisher Scientific, Inc.), were separated on a 10-12% SDS-PAGE gel, electro-transferred to 0.22 μ m polyvinylidene fluoride membranes (EMD Millipore, Billerica, MA, USA) and blocked using 10% bovine serum albumin (BSA) for 1 h at room temperature. Membranes were incubated with the following primary antibodies at 4°C for 14-16 h: Anti-PGC-1 α -N-terminal (1:1,000; cat. no. ab191838), anti-ANP (1:500; cat. no. ab180649), anti-histone H3 (1:1,000; cat. no. ab1791), anti-acyl-coenzyme A dehydrogenase-medium chain (Acadm; 1:10,000; cat. no. ab92461), anti-PPAR- α (1:1,000; cat. no. ab8934; all Abcam), anti-superoxide dismutase 2 (SOD2; 1:1,000; cat. no. sc30080; Santa Cruz Biotechnology, Inc.) and anti- β -actin (cat. no. bs0061R; 1:1,000; BIOS, Beijing, China). Membranes were subsequently incubated with horseradish peroxidase-conjugated goat anti-rabbit IgG secondary antibody (cat. no. sc-2012; 1:5,000; Santa Cruz Biotechnology, Inc.) for 1 h at room temperature. Immunoreactive bands were detected with Pierce enhanced chemiluminescence substrate (Pierce;

Thermo Fisher Scientific, Inc.) and the GeneGnome imaging system (Syngene, Frederick, MD, USA). Bands were quantified using ImageJ software v 1.49 (National Institutes of Health, Bethesda, MD, USA).

Detection of intracellular ATP concentration. An Enhanced ATP Assay kit (Beyotime Institute of Biotechnology) was obtained to measure cellular ATP levels according to the manufacturer's instructions. This kit utilizes a firefly luciferase-based method of detection. Briefly, NRCMs were lysed according to the aforementioned kit at 4°C and centrifuged at 12,000 x g for 5 min. Protein concentration in the supernatant was detected using a BCA protein assay (Thermo Fisher Scientific, Inc.) and the supernatants were mixed with ATP detection working buffer in a white 96-well plate. Luminescence was measured in relative light units using a Multiskan Spectrum SpectraMax M3 (Molecular Devices, LLC, Sunnyvale, CA, USA). ATP levels were expressed as nmol/mg protein.

Measurement of mitochondrial membrane potential (MMP). MMP was detected using a JC-1 fluorescent probe (Beyotime Institute of Biotechnology) according to the manufacturer's instructions. When the MMP increases, JC-1 is aggregated in the matrix of the mitochondria and releases red fluorescence; when the MMP decreases, JC-1 forms monomers and emits green fluorescence. Thus, the ratio of red/green fluorescence reflects the level of relative mitochondrial depolarization. Briefly, cells (10,000/confocal dish) were incubated with JC-1 for 30 min at 37°C and fluorescence images were obtained using an Olympus FV10i confocal microscope (magnification, x10) (Olympus Corporation, Tokyo, Japan). The intensity of the red (excitation wavelength, 490 nm; emission wavelength, 530 nm) and green (excitation wavelength, 525 nm; emission wavelength, 590 nm) fluorescence in NRCMs cultured in a 96-well plate was determined using a SpectraMax M3 microplate reader. Cells treated with 50 mM carbonyl cyanide m-chlorophenylhydrazone at 37°C exhibited a depolarized MMP and were used as a positive control.

Measurement of intracellular ROS levels. A Reactive Oxygen Species Assay kit (Beyotime Institute of Biotechnology) was used to determine ROS levels based on the oxidation of 2',7'-dichlorofluorescein diacetate (DCFH-DA). The experimental procedures were performed strictly according to the manufacturer's guidelines. Following isolation, NRCMs (10,000/confocal dish) were seeded in culture dishes that were observable under a confocal microscope to obtain fluorescence images and fluorescence intensities. Briefly, following treatment with PE and infection with adenovirus expressing either NT-PGC-1 α (Adv-NT-PGC-1 α) or a control vector, cells were harvested and seeded in a 96-well plate at a density of 1×10^5 cells/well. Following incubation with DCFH-DA for 20 min at 37°C, the plate was read at excitation and emission wavelengths of 488 and 525 nm, respectively, using a SpectraMax M3 microplate reader to measure fluorescence intensity. Additionally, NRCMs were visualized with a Olympus FV10i confocal microscope (magnifications, x10 and x60; Olympus Corporation).

Preparation of palmitate (PA)-bovine serum albumin (BSA) and oleic acid (OA)-BSA conjugates. PA and OA were conjugated to fat-free BSA (FA-BSA) as previously described by Choi *et al.* (20). Sodium PA and OA were obtained from Sigma-Aldrich (Merck KGaA). FA-BSA was purchased from Roche Diagnostics. PA and OA were added to 30% BSA at 70°C in a water bath for 30 min. Conjugated molecules were aliquoted and stored at -20°C.

Lipid droplet (LD) staining and detection. NRCMs were incubated with low glucose DMEM (Gibco; Thermo Fisher Scientific, Inc.) containing 1 g/l glucose and 100 μ M OA-BSA conjugate for 24 h at 37°C and subsequently fixed with 4% paraformaldehyde for 30 min at 4°C. Following washing with PBS, cells were stained with 1 μ M BODIPYTM FL C12 lipid probe (Thermo Fisher Scientific, Inc.) and DAPI (Beyotime Institute of Biotechnology) for 30 and 5 min at 37°C, respectively. Cells were subsequently washed with PBS for 5 min three times. Images of fixed cells were captured with an Olympus FV10i confocal laser scanning microscope (magnifications, x10 or x60; Olympus Corporation). BODIPYTM FL C12 was observed as green fluorescence and used to visualize LDs. The number of LDs in each cell was subsequently calculated by Image-Pro Plus 6.0 (Media Cybernetics, Inc., Rockville, MD, USA) for statistical analysis.

Extracellular oxygen consumption. An Extracellular O₂ Consumption Assay kit was purchased from Abcam. The procedure was performed strictly according to the manufacturer's protocol. Briefly, NRCMs were seeded in a black-walled 96-well plate with a clear, flat bottom at a density of 1×10^5 cells/well. Following infection with an Adv-NT-PGC-1 α adenovirus or empty virus, cells were treated with 10 μ M PE or 500 nM MK886 (Abcam) for 48 or 6 h at 37°C, respectively. The medium was subsequently replaced with 150 μ l low-glucose DMEM and 50 μ M PA-BSA, containing 10 μ l Extracellular Oxygen Consumption reagent; control cells were treated with 10 μ l of the low glucose DMEM medium. Following this, pre-warmed (37°C) high-sensitivity mineral oil was rapidly added to limit back diffusion of ambient oxygen,

and the plate was read in a pre-warmed (37°C) SpectraMax M3 microplate reader (excitation, 380 nm; emission, 650 nm). In this assay, the oxygen consumption reagent reflects the oxygen levels in the surrounding medium. As the test material respire, oxygen is depleted in the surrounding environment, which is measured as an increase in the phosphorescence signal.

Statistical analysis. All experiments were performed in triplicate. Data were analyzed by SPSS 20.0 software (IBM Corp., Armonk, NY, USA). Quantitative data were presented as the mean \pm standard error of the mean. A normal distribution test was performed to determine whether parametric or non-parametric tests should be applied. Comparisons of parameters between two experimental groups were performed using a two-tailed t-test, whereas comparisons among three or more groups were performed using two-way analysis of variance, followed by the Least Significant Difference test or Dunnett's T3 test for multiple comparisons. $P < 0.05$ was considered to indicate a statistically significant difference.

Results

NT-PGC-1 α is predominantly expressed in the cytoplasm of NRCMs. NRCMs were infected with mCherry-Adv-NT-PGC-1 α for 24 h, stained with Hoechst 33258 for 10 min and observed by confocal microscopy to examine the subcellular localization of NT-PGC-1 α . Immunofluorescence staining of NRCMs was performed to detect total PGC-1 α , including FL-PGC-1 α and NT-PGC-1 α . NT-PGC-1 α was primarily located in the cytoplasm, with a small amount distributed in the nucleus (Fig. 1A), whereas endogenous PGC-1 α was predominantly located in the nucleus (Fig. 1B). In addition, western blot analysis of cytoplasmic and nuclear protein extracts from mouse heart tissues demonstrated that the distribution of NT-PGC-1 α was markedly different from that of PGC-1 α (Fig. 1C).

NT-PGC-1 α overexpression attenuates reductions in MMP, ATP and ROS generation. Cells were infected with Adv-NT-PGC-1 α or control adenovirus and subsequently exposed to 10 μ M PE or 1 μ M Ang II for 48 h. Intracellular ATP concentrations were measured using a microplate reader. Cells incubated with PE (4.851 ± 0.535 nmol/mg; $n=8$) or Ang II (3.931 ± 0.685 nmol/mg; $n=8$) had significantly reduced ATP levels compared with cells infected with the control adenovirus alone (9.100 ± 0.745 nmol/mg; $P < 0.01$; Fig. 2A). This impairment in ATP generation was significantly alleviated by NT-PGC-1 α overexpression induced by Adv-NT-PGC-1 α infection, when compared with PE treatment (4.851 ± 0.535 vs. 7.288 ± 0.519 nmol/mg; $n=7-8$; $P < 0.05$) or Ang II treatment (3.931 ± 0.685 vs. 6.588 ± 0.453 nmol/mg; $n=8$; $P < 0.01$) in the control adenovirus groups (Fig. 2A).

MMP and ROS generation were assessed to further investigate the effect of NT-PGC-1 α on mitochondrial function. Following infection with Adv-NT-PGC-1 α and incubation of NRCMs with PE, cells were treated with either JC-1 or DCFH-DA. The relative MMP levels, indicated by the red/green fluorescence ratio, were significantly decreased in the PE+vehicle group (0.504 ± 0.035 ; $n=12$) when compared with that of the vehicle control (1.000 ± 0.033 ; $n=12$; $P < 0.01$). Adv-NT-PGC-1 α

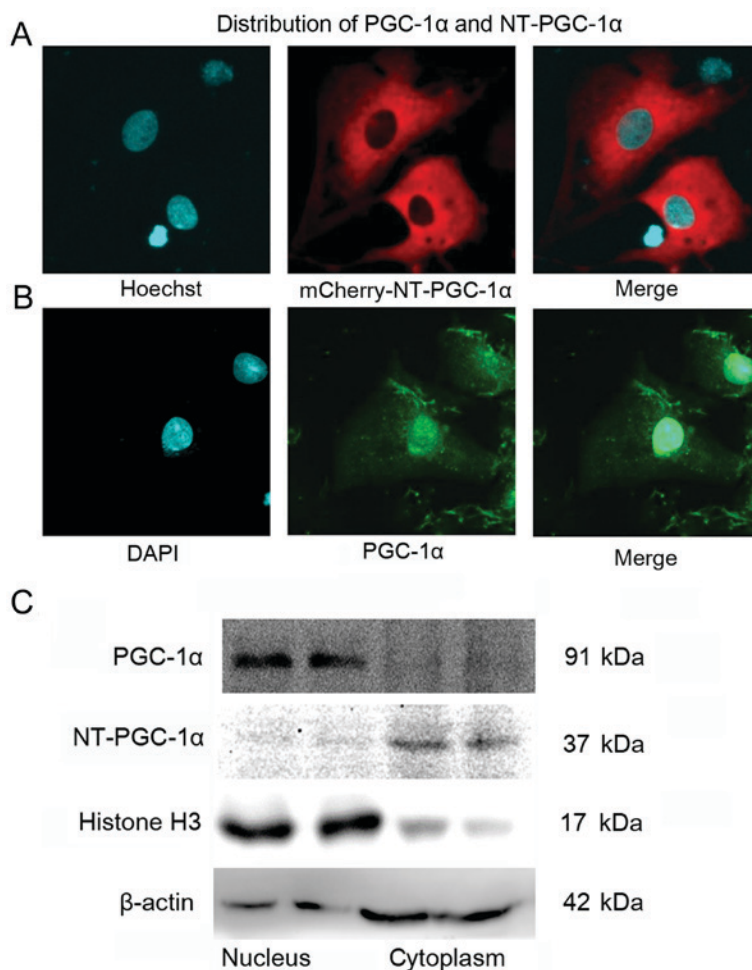


Figure 1. Subcellular localization of NT-PGC-1 α . (A) NRCMs were infected with mCherry-NT-PGC-1 α adenovirus and observed by confocal microscopy. NT-PGC-1 α was primarily located in the cytoplasm. (B) Immunofluorescence staining revealed the different distribution patterns for endogenous total PGC-1 α and NT-PGC-1 α . (C) Western blot analysis of nuclear and cytoplasmic fractions demonstrated the subcellular location of endogenous PGC-1 α and NT-PGC-1 α expression. Experiments were repeated three times. NRCMs, neonatal rat cardiomyocytes; PGC-1 α , peroxisome proliferator-activated receptor- γ coactivator-1 α ; NT, N-terminal truncated.

infection in PE-treated cells significantly reversed the effect of PE treatment on MMP levels (0.679 ± 0.029 vs. 0.504 ± 0.035 ; $n=12$; $P<0.01$; Fig. 2B and C). Additionally, PE resulted in increased ROS levels compared with the corresponding empty virus control (1.619 ± 0.059 vs. 1.000 ± 0.069 ; $n=16$; $P<0.01$), whereas NT-PGC-1 α overexpression inhibited the ROS generation induced by PE (1.437 ± 0.063 vs. 1.619 ± 0.059 ; $n=16$; $P<0.05$; Fig. 2D and E). These results indicated that NT-PGC-1 α may have improved mitochondrial function.

NT-PGC-1 α increases fatty acid metabolism-associated gene expression. RT-qPCR demonstrated that Adv-NT-PGC-1 α infection effectively increased NT-PGC-1 α expression when compared with the empty vehicle control ($P<0.01$; Fig. 3A). NT-PGC-1 α overexpression significantly enhanced the transcription of fatty acid metabolism-associated genes (Fig. 3B), including carnitine palmitoyltransferase 1b (CPT1b; 1.000 ± 0.208 vs. 8.603 ± 2.822 ; $n=8$; $P<0.05$), carnitine palmitoyltransferase 2 (CPT-2; 1.000 ± 0.225 vs. 2.846 ± 0.542 ; $n=8$; $P<0.01$), acyl-coenzyme A dehydrogenase-very long chain (Acadvl; 1.000 ± 0.337 vs. 7.027 ± 2.144 ; $n=8$; $P<0.05$), Acadm (1.000 ± 0.150 vs. 2.712 ± 0.607 ; $n=8$; $P<0.05$), pyruvate dehydrogenase kinase 4 (PDK4; 1.000 ± 0.228 vs. 7.717 ± 2.072 ; $n=8$; $P<0.01$), PPAR- α

(1.000 ± 0.306 vs. 6.309 ± 1.518 ; $n=6$; $P<0.05$) and superoxide dismutase 3 (SOD3; 1.000 ± 0.147 vs. 5.565 ± 1.972 ; $n=8$; $P<0.05$). However, no significant differences were detected in the levels of SOD2 (1.000 ± 0.123 vs. 3.925 ± 1.414 ; $n=8$; $P=0.058$) and FL-PGC-1 α (1.000 ± 0.134 vs. 2.402 ± 0.857 ; $n=8$).

Cells were treated with MK886, a fatty acid metabolism inhibitor, to investigate the potential pathways by which NT-PGC-1 α overexpression may have altered the expression of these genes. MK886 is a PPAR- α antagonist and was demonstrated to inhibit the expression of PPAR- α and its downstream proteins CPT-2 and Acadm, as well as PGC-1 α , in a dose-dependent manner (Fig. 3C and D). The western blot results indicated that the expression levels of CPT-2 (0.505 ± 0.019 vs. 0.239 ± 0.034 for β -actin; $n=5$; $P<0.01$) were significantly decreased in cells exposed to PE, and Acadm (0.511 ± 0.078 vs. 0.303 ± 0.012 for β -actin; $n=5$; $P<0.01$) also decreased when exposed to PE (Fig. 3E and G; Lanes 1 and 3), and these effects were reversed by NT-PGC-1 α overexpression (CPT-2, 0.377 ± 0.026 ; $P<0.01$; Acadm, 0.498 ± 0.032 ; $P<0.05$; Fig. 3E and G; Lane 4). In addition, NT-PGC-1 α overexpression also reversed the PE-induced increase detected in atrial natriuretic peptide (ANP) levels ($P<0.01$; Fig. 3E and G; Lane 4). Additionally, the expression levels of NT-PGC-1 α

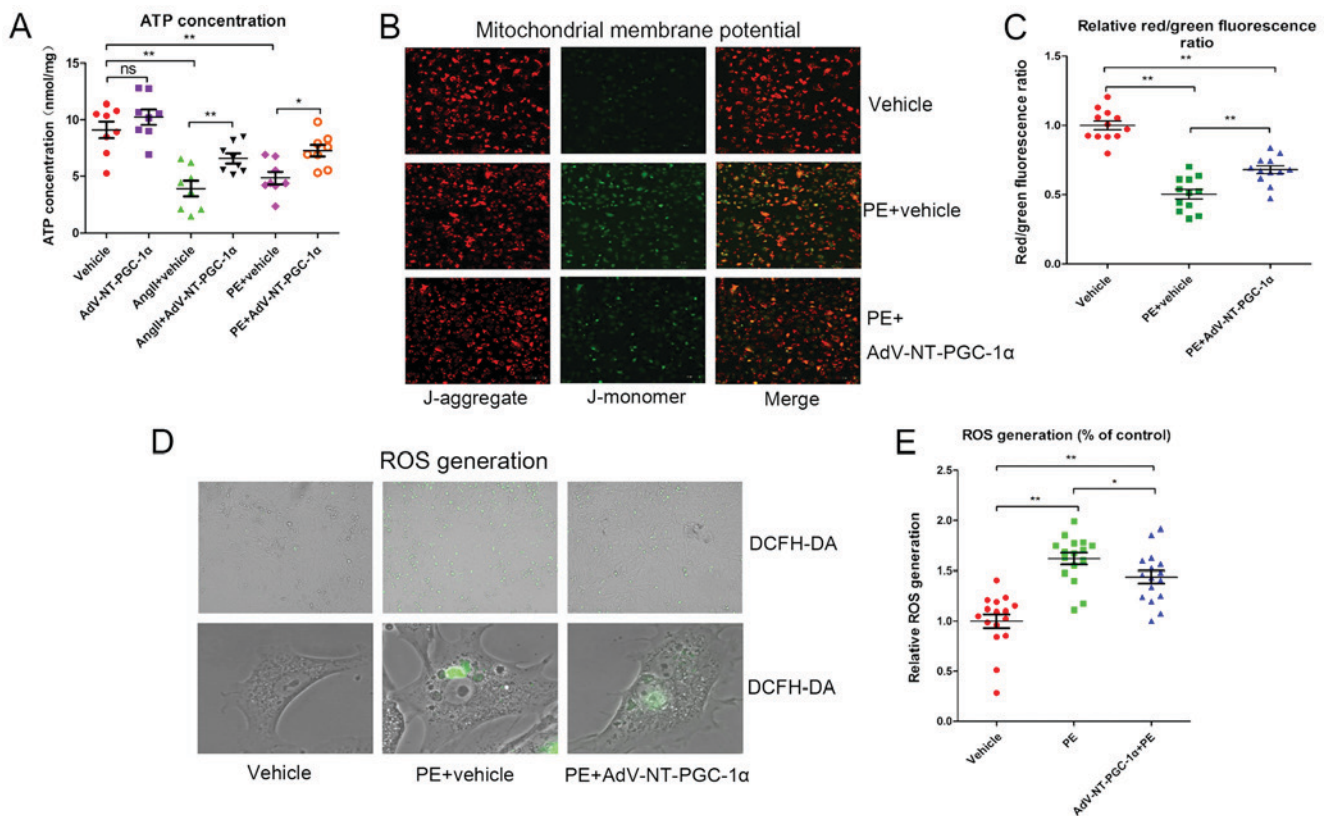


Figure 2. Effect of NT-PGC-1 α overexpression on MMP, ATP and ROS generation in cells infected with NT-PGC-1 α or control adenovirus and exposed to PE or Ang II. (A) Intracellular ATP levels (n=7-8 per group). (B) MMP was detected using the JC-1 assay and (C) the ratio of red/green fluorescence was calculated (n=12 per group). (D) ROS generation was measured by DCFH-DA fluorescence and (E) relative fluorescence levels were calculated (n=16 per group). *P<0.05 and **P<0.01, as indicated. Adv, adenovirus; NT-PGC-1 α , N-terminal truncated peroxisome proliferator-activated receptor- γ coactivator-1 α ; MMP, mitochondrial membrane potential; ATP, adenosine 5'-triphosphate; ROS, reactive oxygen species; DCFH-DA, dichlorofluorescein diacetate.

in different groups were evaluated to ensure the success of Adv-NT-PGC-1 α infection (Fig. 3F). These effects of NT-PGC- α overexpression on fatty acid metabolism were attenuated by MK886 (Fig. 3E and G; between lanes 1 and 2; lanes 5 and 6).

NT-PGC-1 α overexpression decreases LD accumulation in high lipid medium. NRCMs overexpressing NT-PGC-1 α were incubated with OA-BSA for 24 h and subsequently treated with MK886 for 6 h to investigate the mechanism by which NT-PGC-1 α regulated fatty acid metabolism. Notably, the number of LDs (Fig. 4) was significantly increased in cells incubated with OA-BSA compared with vehicle control cells (111.10 \pm 9.86 vs. 1.73 \pm 0.48; n=30 and 27, respectively; P<0.01; Fig. 4A, B and E). NT-PGC-1 α overexpression significantly decreased the number of LDs compared with the OA-BSA+vehicle group (61.90 \pm 8.69 vs. 111.10 \pm 9.86; n=50 and 30, respectively; P<0.01; Fig. 4B, C and E). As expected, the effect of NT-PGC-1 α was markedly reduced in cells exposed to MK886 (Fig. 4C, D and E; P<0.01). Taken together, these results demonstrated that NT-PGC-1 α overexpression decreased lipid accumulation in NRCMs, indicating a role for NT-PGC-1 α in fatty acid metabolism.

NT-PGC-1 α overexpression increases the oxygen consumption in high lipid medium. Based on results obtained by LD staining and western blot analyses of fatty

acid metabolism-associated enzymes, the present study investigated the oxygen consumption of NRCMs in high lipid medium (50 μ M PA). NT-PGC-1 α -overexpressing NRCMs were stimulated with PE or MK886 and extracellular oxygen consumption rates were analyzed. As indicated in Fig. 5A, oxygen consumption steadily increased in control empty virus cells during the monitoring period, whereas cells infected with Adv-NT-PGC-1 α exhibited a significant increase in oxygen consumption. In addition, NT-PGC-1 α -overexpressing NRCMs exposed to 10 μ M PE or 500 nM MK886 displayed an increasing trend in oxygen consumption, that was slower compared with NT-PGC-1 α -overexpressing NRCMs that had not been exposed to PE or MK886. Furthermore, PE or MK886 exposure reduced oxygen consumption in cells lacking NT-PGC-1 α overexpression, with only a marginal increase observed over time (Fig. 5A). Further comparison of oxygen consumption among the different groups at the end of the observational period revealed significant differences in consumption between the vehicle (989.88 \pm 147.89) and PE+vehicle (362.00 \pm 64.54.05; n=7-8; P<0.01) and Adv-NT-PGC-1 α (1,629.82 \pm 228.42; n=8; P<0.01) groups. In addition, consumption was significantly different between the PE+vehicle (362.00 \pm 64.54.05) and PE+Adv-NT-PGC-1 α (1,026.82 \pm 170.29; n=8; P<0.01) groups, as well as between the MK886+vehicle (546.84 \pm 89.08) and MK886+Adv-NT-PGC-1 α (1,133.90 \pm 164.19; n=7-8; P<0.05) groups (Fig. 5B).

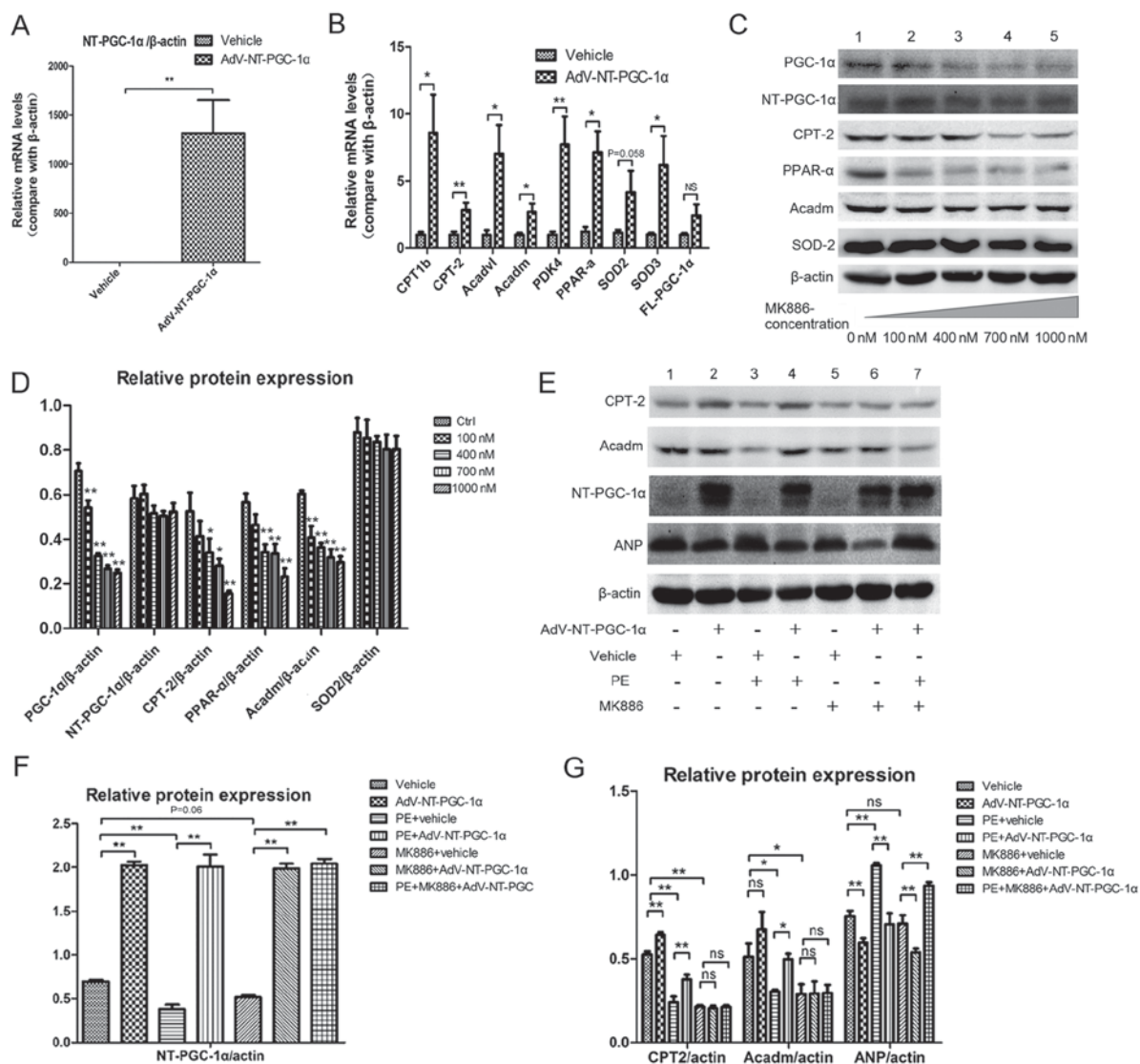


Figure 3. NT-PGC-1 α overexpression increases fatty acid metabolism-associated gene expression. (A) NT-PGC-1 α overexpression in NRCMs induced by adenoviral infection (n=6-8 per group). (B) Effect of NT-PGC-1 α overexpression on the expression of downstream target genes, including enzymes involved in fatty acid metabolism and anti-oxidant enzymes (n=6-8 per group). (C) Alterations in the expression of PGC-1 α , NT-PGC-1 α , CPT-2, PPAR- α , Acadm and SOD2 in response to treatment with MK886, a PPAR- α inhibitor. (D) Quantification of western blot results by densitometry (n=3-5 per group). (E-G) Effect of NT-PGC-1 α overexpression, PE and MK886 (500 nM) on fatty acid metabolism-associated protein expression (n=5 per group). *P<0.05 and **P<0.01, as indicated or compared with the control. AdV, adenovirus; NT, N-terminal truncated; PGC-1 α , peroxisome proliferator-activated receptor- γ coactivator-1 α ; CPT-2, carnitine palmitoyltransferase 2; PPAR- α , peroxisome proliferator-activated receptor α ; Acadm, medium-chain specific acyl-coenzyme A dehydrogenase, mitochondrial; SOD2, superoxide dismutase 2; PE, phenylephrine; ns, not significant.

Discussion

In the present study, the role of NT-PGC-1 α in NRCMs was examined. It was demonstrated that NT-PGC-1 α influenced MMP and fatty acid metabolism in cardiomyocytes. NT-PGC-1 α is primarily located in the cytoplasm, unlike FL-PGC-1 α , and has been reported to regulate fatty acid metabolism in adipose tissue in the absence of FL-PGC-1 α (18,23). Consistent with these results, the present study examined the cellular distribution of FL-PGC-1 α and NT-PGC-1 α by immunofluorescence and western blotting to determine that NT-PGC-1 α was primarily expressed in the cytoplasm and may perform similar roles in fatty acid metabolism in NRCMs. Previous studies on the effects of NT-PGC-1 α have primarily been examined in adipocytes or skeletal muscle cells (24,25); however, limited reports have investigated the expression of NT-PGC-1 α in

human heart tissue. Thus, the present study further explored the effects of NT-PGC-1 α in cardiomyocytes.

ATP and ROS production, as well as the MMP were detected to examine the function of NT-PGC-1 α in NRCMs. NT-PGC-1 α overexpression alleviated PE- or Ang II-induced reductions in ATP production and PE-induced ROS generation. These effects may have contributed to its role in mitochondrial function improvement, as NT-PGC-1 α also reversed PE-induced MMP impairment. PE and Ang II are G-protein-coupled receptor agonists, which have potent pro-hypertrophic effects in the heart, leading to increases in ANP and brain natriuretic peptide, which are indicators of heart failure or heart impairment (26). Furthermore, they are well-known stimulants for establishing cardiac hypertrophy and heart failure experimental models (27), despite also exerting critical effects in blood pressure maintenance.

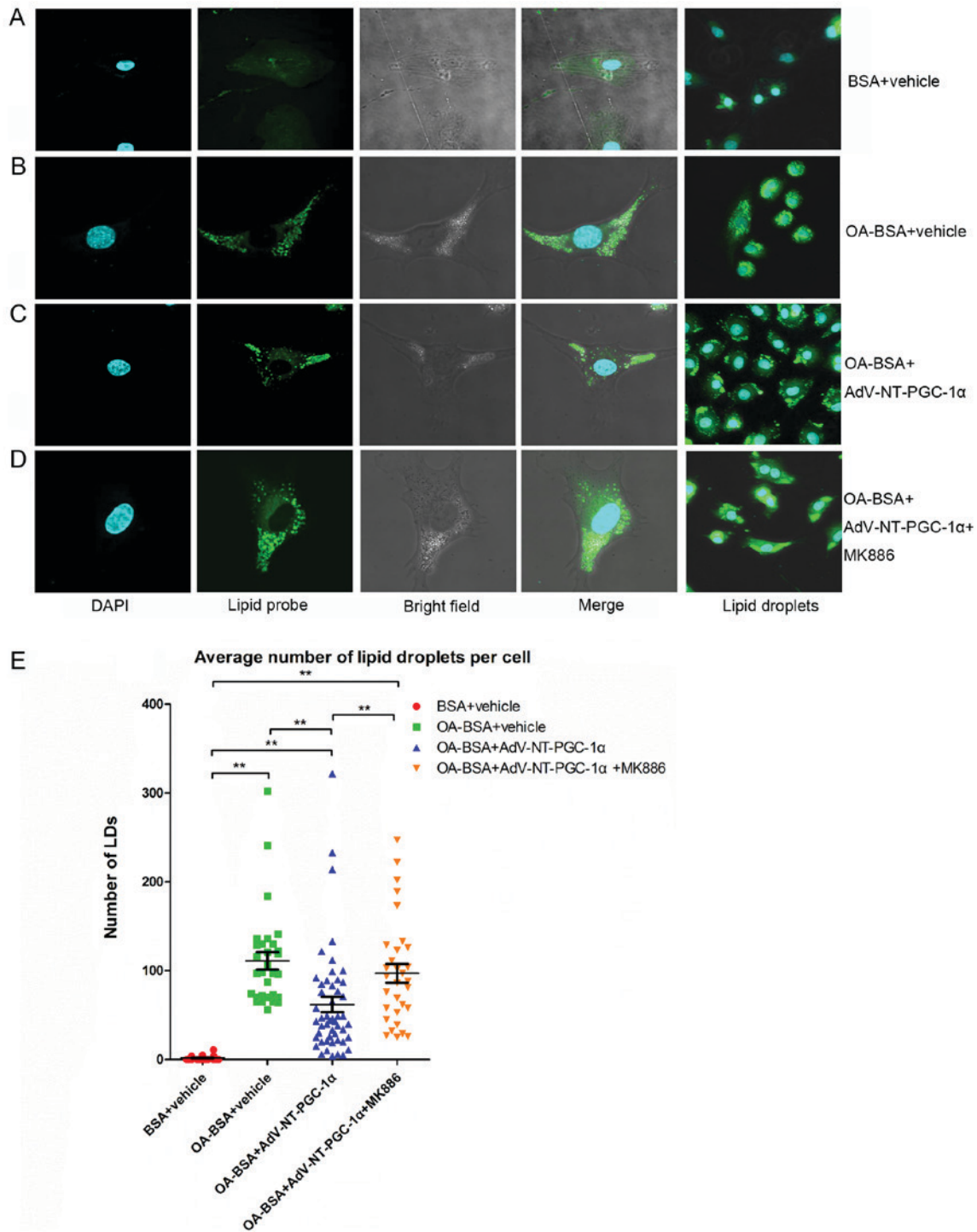


Figure 4. NT-PGC-1 α overexpression reduces LD accumulation in NRCMs. Representative images of LD staining of NRCMs cultured in high lipid medium from (A) the BSA+vehicle group, (B) OA-BSA+vehicle group, (C) OA-BSA+AdV-NT-PGC-1 α group and (D) OA-BSA+AdV-NT-PGC-1 α +MK886 group. (E) NT-PGC-1 α overexpression reduced LD accumulation in NRCMs. The number of LDs in each group was counted. ** $P < 0.01$, as indicated. BSA+vehicle, $n = 27$; OA-BSA+vehicle, $n = 30$; OA-BSA+AdV-NT-PGC-1 α , $n = 50$ and OA-BSA+AdV-NT-PGC-1 α +MK886, $n = 31$. AdV, adenovirus; NT-PGC-1 α , N-terminal truncated peroxisome proliferator-activated receptor- γ coactivator-1 α ; LDs, lipid droplets; NRCMs, neonatal rat cardiomyocytes; OA, oleic acid; BSA, bovine serum albumin.

Additionally, PE may inhibit the expression of PPAR- α (28), which is associated with energy metabolic dysfunction in heart disease. Therefore, it was postulated that NT-PGC-1 α overexpression may have ameliorated the impairments in mitochondrial function induced by PE and Ang II in the present study.

Although NT-PGC-1 α has a structure similar to FL-PGC-1 α , FL-PGC-1 α has anti-oxidative effects and is

versatile in transcription (17,29). Thus, NT-PGC-1 α may have a similar function to PGC-1 α and exert its effects by associating with transcription factors via its nuclear domain in the nucleus, or may be directly associated with mitochondria via protein interactions.

To the best of our knowledge, the role of NT-PGC-1 α in NRCM fatty acid metabolism has not been previously investigated. However, in a recent study focused on obesity,

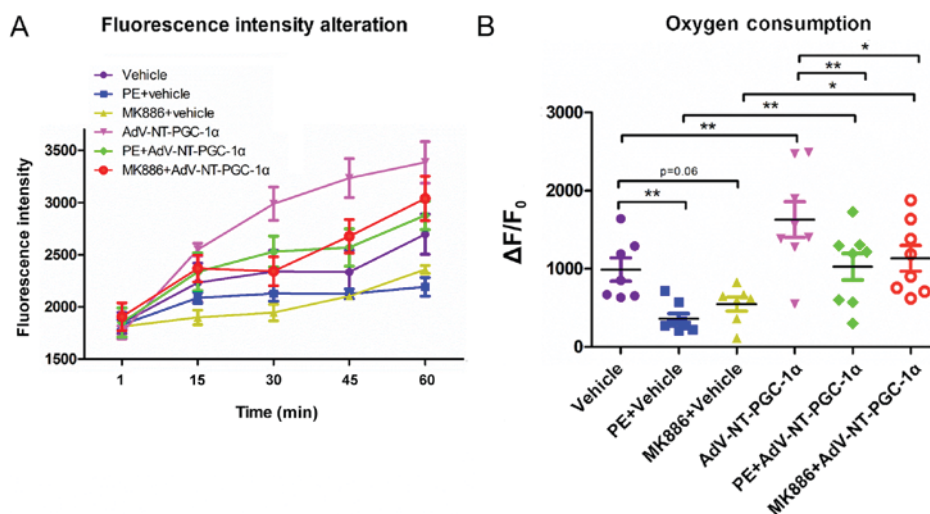


Figure 5. NT-PGC-1 α overexpression in NRCMs increases extracellular oxygen consumption. (A) Variations in oxygen consumption in response to different stimuli. (B) Oxygen consumption following 1 h compared with the baseline (n=7-8 per group). *P<0.05 and **P<0.01, as indicated. NT-PGC-1 α , N-terminal truncated peroxisome proliferator-activated receptor- γ coactivator-1 α ; NRCMs, neonatal rat cardiomyocytes; PE, phenylephrine; Adv, adenovirus; F, fluorescence.

NT-PGC-1 α was reported to have a profound impact on FAO in mice (23). In addition, Zhang *et al* (17) observed that NT-PGC-1 α overexpression upregulates the expression of its downstream target CPT-2 (17). Furthermore, crosstalk between NT-PGC-1 α and phosphatase and tensin homolog-induced putative kinase 1 (PINK1) is involved in FAO (30), and PINK1 silencing impairs PGC-1 α -associated lipid metabolism (20). Thus, NT-PGC-1 α is important in fatty acid metabolism and may ameliorate the metabolic deficits observed in patients with cardiac hypertrophy and heart failure.

In support of this hypothesis, the present study demonstrated that NT-PGC-1 α overexpression increased the mRNA expression of PPAR- α -associated genes and alleviated PE-induced reductions in CPT-2 and Acadm expression, enzymes that are involved in transferring fatty acids to mitochondria and initiating the mitochondrial fatty acid β -oxidation pathway. In the present study, NT-PGC-1 α -overexpressing NRCMs were treated with MK886, a lipoxygenase inhibitor that antagonizes PPAR- α activity (31). As expected, MK886 reduced the effect of NT-PGC-1 α on the expression of fatty acid metabolism-associated proteins. Thus, NT-PGC-1 α may have exerted metabolic effects, as well as influencing the PPAR- α signaling pathway activity to an extent.

Furthermore, the effects of NT-PGC-1 α overexpression on free fatty acid (FFA) metabolism were examined. LDs accumulated in NRCMs when cells were exposed to OA-BSA, whereas NT-PGC-1 α overexpression reduced the number of LDs that accumulated in cells. In addition, the LD number increased in NRCMs infected with Adv-NT-PGC-1 α and treated with MK886. Strategies that enhance FAO increase the levels of FFA and β -oxidation (32); however, as FFA content in the culture medium was at a constant level, the fatty acid was mostly from exogenous sources rather than lipid mobilization in the present study. Based on these results, NT-PGC-1 α may alleviate the lipotoxicity of FFA by enhancing its metabolism, rather than via lipid mobilization.

To further investigate the function of NT-PGC-1 α in fatty acid metabolism, the present study measured oxygen

consumption in NT-PGC-1 α -overexpressing NRCMs exposed to PE and/or MK886 in a high lipid medium. NT-PGC-1 α overexpression resulted in increased oxygen consumption, consistent with the findings of protein expression levels. Therefore, NT-PGC-1 α may function by shuttling into the nucleus and activating the associated signaling pathway, or it may originate and function in the nucleus. It is also possible that it directly participates in crosstalk with mitochondria in the cytoplasm. If NT-PGC-1 α functions in the nucleus, then forced NT-PGC-1 α nuclear translocation would likely enhance its function; a cyclic adenosine monophosphate (cAMP) analog was reported to activate PGC-1 α and increase the nuclear localization of NT-PGC-1 α (17), and the function of cAMP in myocardial contractility is well established (33). However, additional studies are required to verify whether nuclear NT-PGC-1 α acts as an effector molecule in response to cAMP stimulation. Recent research demonstrated that NT-PGC-1 α directly interacts with mitochondria (34); therefore, it may exert effects in the nucleus and the cytoplasm. Combined with the findings of these previous reports, the present study validated that NT-PGC-1 α has several roles in fatty acid metabolism in various cell types, and may have broad applications in the treatment of obesity, heart failure and atherosclerosis.

There are certain limitations and drawbacks to the present study. First, endogenous NT-PGC-1 α was not detected by immunofluorescence; FL-PGC-1 α contains all of the antigen epitopes in NT-PGC-1 α , whereas NT-PGC-1 α lacks the C-terminal epitopes of FL-PGC-1 α (35). Thus, a N-terminal PGC-1 α antibody would detect NT-PGC-1 α and FL-PGC-1 α , while a C-terminal PGC-1 α antibody would only detect FL-PGC-1 α . Therefore, evaluation of NT-PGC-1 α expression in NRCMs without transfection failed due to antibody limitations, preventing the immunofluorescent detection of NT-PGC-1 α . Therefore, the most reliable way to accurately detect endogenous NT-PGC-1 α at present may be to separate cytoplasmic and nuclear proteins. Secondly, FAO was not examined directly, and the results of western blotting, LD accumulation and oxygen consumption only provide indirect

evidence. Furthermore, application of small interfering RNA rather than an inhibitor to interfere with PPAR- α expression may provide more conclusive data to support the proposed pathway of NT-PGC-1 α . In addition, the roles of NT-PGC-1 α in the cytoplasm and its effects in animal heart tissue require further exploration.

In conclusion, the present study demonstrated that NT-PGC-1 α alleviated PE-induced mitochondrial function impairment and influenced fatty acid metabolism in NRCMs, likely through the PPAR- α -associated signaling pathway. Thus, NT-PGC-1 α may provide a promising target for the treatment of cardiac hypertrophy and heart failure.

Acknowledgements

Not applicable.

Funding

The present study was supported by the National Natural Science Foundation of China (grant no. 81270320).

Availability of data and materials

The datasets used and/or analyzed during the current study are available from the corresponding author on reasonable request.

Authors' contributions

DX, HR and QZe made substantial contributions to the design of the present study experiments. QZh and WL conducted cell cultures. ZL, JH and WC performed experiments and analyzed data. ZL, JH and QZh produced the figures. ZL, JH and WL prepared the manuscript. All authors read and approved the final version of the manuscript.

Ethics approval and consent to participate

The present study was approved by the Southern Medical University review board and the animal protocols used complied with the Guide for the Care and Use of Laboratory Animals (21).

Patient consent for publication

Not applicable.

Competing interests

The authors declare that they have no competing interests.

References

- Neubauer S: The failing heart-an engine out of fuel. *N Engl J Med* 356: 1140-1151, 2007.
- Kong X, Banks A, Liu T, Kazak L, Rao RR, Cohen P, Wang X, Yu S, Lo JC, Tseng YH, *et al*: IRF4 is a key thermogenic transcriptional partner of PGC-1 α . *Cell* 158: 69-83, 2014.
- Huang TY, Zheng D, Houmard JA, Braut JJ, Hickner RC and Cortright RN: Overexpression of PGC-1 α increases peroxisomal and mitochondrial fatty acid oxidation in human primary myotubes. *Am J Physiol Endocrinol Metab* 331-2016, 2017.
- Wu Z, Puigserver P, Andersson U, Zhang C, Adelmant G, Mootha V, Troy A, Cinti S, Lowell B, Scarpulla RC and Spiegelman BM: Mechanisms controlling mitochondrial biogenesis and respiration through the thermogenic coactivator PGC-1. *Cell* 98: 115-124, 1999.
- Depre C, Vanoverschelde JL and Taegtmeyer H: Glucose for the heart. *Circulation* 99: 578-588, 1999.
- Arumugam S, Sreedhar R, Thandavarayan RA, Karuppagounder V and Watanabe K: Targeting fatty acid metabolism in heart failure: Is it a suitable therapeutic approach? *Drug Discov Today* 21: 1003-1008, 2016.
- Lin J, Wu PH, Tarr PT, Lindenberg KS, St-Pierre J, Zhang CY, Mootha VK, Jager S, Vianna CR, Reznick RM, *et al*: Defects in adaptive energy metabolism with CNS-linked hyperactivity in PGC-1 α null mice. *Cell* 119: 121-135, 2004.
- Leone TC, Lehman JJ, Finck BN, Schaeffer PJ, Wende AR, Boudina S, Courtois M, Wozniak DF, Sambandam N, Bernal-Mizrachi C, *et al*: PGC-1 α deficiency causes multi-system energy metabolic derangements: Muscle dysfunction, abnormal weight control and hepatic steatosis. *PLoS Biol* 3: e101, 2005.
- Karamanlidis G, Garcia-Menendez L, Kolwicz SJ, Lee CF and Tian R: Promoting PGC-1 α -driven mitochondrial biogenesis is detrimental in pressure-overloaded mouse hearts. *Am J Physiol Heart Circ Physiol* 307: H1307-H1316, 2014.
- LeBleu VS, O'Connell JT, Gonzalez HK, Wikman H, Pantel K, Haigis MC, de Carvalho FM, Damascena A, Domingos CL, Rocha RM, *et al*: PGC-1 α mediates mitochondrial biogenesis and oxidative phosphorylation in cancer cells to promote metastasis. *Nat Cell Biol* 16: 992-1003, 1-15, 2014.
- Russell LK, Mansfield CM, Lehman JJ, Kovacs A, Courtois M, Saffitz JE, Medeiros DM, Valencik ML, McDonald JA and Kelly DP: Cardiac-specific induction of the transcriptional coactivator peroxisome proliferator-activated receptor gamma coactivator-1 α promotes mitochondrial biogenesis and reversible cardiomyopathy in a developmental stage-dependent manner. *Circ Res* 94: 525-533, 2004.
- Pereira RO, Wende AR, Crum A, Hunter D, Olsen CD, Rawlings T, Riehle C, Ward WF and Abel ED: Maintaining PGC-1 α expression following pressure overload-induced cardiac hypertrophy preserves angiogenesis but not contractile or mitochondrial function. *FASEB J* 28: 3691-3702, 2014.
- Xie J, Cui K, Hao H, Zhang Y, Lin H, Chen Z, Huang X, Cao S, Liao W, Bin J, *et al*: Acute hyperglycemia suppresses left ventricular diastolic function and inhibits autophagic flux in mice under prohypertrophic stimulation. *Cardiovasc Diabetol* 15: 136, 2016.
- Li Y, Li J, Hou Z, Yu Y and Yu B: KLF5 overexpression attenuates cardiomyocyte inflammation induced by oxygen-glucose deprivation/reperfusion through the PPAR γ /PGC-1 α /TNF- α signaling pathway. *Biomed Pharmacother* 84: 940-946, 2016.
- Gundewar S, Calvert JW, Jha S, Toedt-Pingel I, Ji SY, Nunez D, Ramachandran A, Anaya-Cisneros M, Tian R and Lefer DJ: Activation of AMP-activated protein kinase by metformin improves left ventricular function and survival in heart failure. *Circ Res* 104: 403-411, 2009.
- Patten IS and Arany Z: PGC-1 coactivators in the cardiovascular system. *Trends Endocrinol Metab* 23: 90-97, 2012.
- Zhang Y, Huypens P, Adamson AW, Chang JS, Henagan TM, Boudreau A, Lenard NR, Burk D, Klein J, Perwitz N, *et al*: Alternative mRNA splicing produces a novel biologically active short isoform of PGC-1 α . *J Biol Chem* 284: 32813-32826, 2009.
- Trausch-Azar J, Leone TC, Kelly DP and Schwartz AL: Ubiquitin proteasome-dependent degradation of the transcriptional coactivator PGC-1 α via the N-terminal pathway. *J Biol Chem* 285: 40192-40200, 2010.
- Chang JS, Huypens P, Zhang Y, Black C, Kralli A and Gettys TW: Regulation of NT-PGC-1 α subcellular localization and function by protein kinase A-dependent modulation of nuclear export by CRM1. *J Biol Chem* 285: 18039-18050, 2010.
- Choi J, Ravipati A, Nimmagadda V, Schubert M, Castellani RJ and Russell JW: Potential roles of PINK1 for increased PGC-1 α -mediated mitochondrial fatty acid oxidation and their associations with Alzheimer disease and diabetes. *Mitochondrion* 18: 41-48, 2014.
- Guide for the Care and Use of Laboratory Animals, 8th Edition, 2011, <https://grants.nih.gov/grants/olaw/Guide-for-the-Care-and-Use-of-Laboratory-Animals.pdf>.

22. Livak KJ and Schmittgen TD: Analysis of relative gene expression data using real-time quantitative PCR and the 2(-Delta Delta C(T)) Method. *Methods* 25: 402-408, 2001.
23. Kim J, Fernand VE, Henagan TM, Shin J, Huypens P, Newman S, Gettys TW and Chang JS: Regulation of brown and white adipocyte transcriptome by the transcriptional coactivator NT-PGC-1alpha. *PLoS One* 11: e159990, 2016.
24. Jun HJ, Joshi Y, Patil Y, Noland RC and Chang JS: NT-PGC-1alpha activation attenuates high-fat diet-induced obesity by enhancing brown fat thermogenesis and adipose tissue oxidative metabolism. *Diabetes* 63: 3615-3625, 2014.
25. Popov DV, Bachinin AV, Lysenko EA, Miller TF and Vinogradova OL: Exercise-induced expression of peroxisome proliferator-activated receptor γ coactivator-1 α isoforms in skeletal muscle of endurance-trained males. *J Physiol Sci* 64: 317-323, 2014.
26. Keys JR, Zhou RH, Harris DM, Druckman CA and Eckhart AD: Vascular smooth muscle overexpression of G protein-coupled receptor kinase 5 elevates blood pressure, which segregates with sex and is dependent on Gi-mediated signaling. *Circulation* 112: 1145-1153, 2005.
27. Schlegel P, Reinkober J, Meinhardt E, Tscheschner H, Gao E, Schumacher SM, Yuan A, Backs J, Most P, Wieland T, *et al*: G protein-coupled receptor kinase 2 promotes cardiac hypertrophy. *PLoS One* 12: e182110, 2017.
28. Huang Q, Huang J, Zeng Z, Luo J, Liu P, Chen S, Liu B, Pan X, Zang L and Zhou S: Effects of ERK1/2/PPARalpha/SCAD signal pathways on cardiomyocyte hypertrophy induced by insulin-like growth factor 1 and phenylephrine. *Life Sci* 124: 41-49, 2015.
29. Geng T, Li P, Yin X and Yan Z: PGC-1alpha promotes nitric oxide antioxidant defenses and inhibits FOXO signaling against cardiac cachexia in mice. *Am J Pathol* 178: 1738-1748, 2011.
30. Choi J, Batchu VV, Schubert M, Castellani RJ and Russell JW: A novel PGC-1alpha isoform in brain localizes to mitochondria and associates with PINK1 and VDAC. *Biochem Biophys Res Commun* 435: 671-677, 2013.
31. Kehrer JP, Biswal SS, La E, Thuillier P, Datta K, Fischer SM and Vanden HJ: Inhibition of peroxisome-proliferator-activated receptor (PPAR)alpha by MK886. *Biochem J* 356: 899-906, 2001.
32. Pascual F and Coleman RA: Fuel availability and fate in cardiac metabolism: A tale of two substrates. *Biochim Biophys Acta* 1861: 1425-1433, 2016.
33. Beca S, Ahmad F, Shen W, Liu J, Makary S, Polidovitch N, Sun J, Hockman S, Chung YW, Movsesian M, *et al*: Phosphodiesterase type 3A regulates basal myocardial contractility through interacting with sarcoplasmic reticulum calcium ATPase type 2a signaling complexes in mouse heart. *Circ Res* 112: 289-297, 2013.
34. Chang JS and Ha K: An unexpected role for the transcriptional coactivator isoform NT-PGC-1alpha in the regulation of mitochondrial respiration in brown adipocytes. *J Biol Chem* 292: 9958-9966, 2017.
35. Villena JA: New insights into PGC-1 coactivators: Redefining their role in the regulation of mitochondrial function and beyond. *FEBS J* 282: 647-672, 2015.



This work is licensed under a Creative Commons Attribution-NonCommercial-NoDerivatives 4.0 International (CC BY-NC-ND 4.0) License.